Supporting Information for

Single-Component Supported Lipid Bilayers Probed Using Broadband Nonlinear Optics

Laura L. Olenick,[a] Hilary M. Chase,[a] Li Fu,[b,c] Yun Zhang,[b,d] Alicia C. McGeachy,[a] Merve Dogangun,[a] Stephanie R. Walter,[a] Hong-fei Wang,[e] and Franz M. Geiger[a*]

[a]Department of Chemistry, Northwestern University, Evanston, IL 60208, USA, [b]William R. Wiley Environmental Molecular Sciences Laboratory, Pacific Northwest National Laboratory, Richland, WA 99352, United States, [c]Sanofi-Genzyme, Framingham, MA, 01701, [d]Institute of Optics and Electronics, Chinese Academy of Sciences, Chengdu, Sichuan, 610209, China, and [e]Department of Chemistry, Fudan University, Shanghai 200433, China

1. Orientation Analysis of Alkyl Chain Terminal CH_3 of 9:1 DMPC/DMPG in D_2O

SFG spectroscopy is excellent for probing the molecular orientation of a species at an interface. In these SFG spectroscopy experiments, we are able to control the polarization of the IR, visible, and SFG light fields and to isolate various $\chi^{(2)}$ tensor elements. Specifically, by probing a 9:1 DMPC/DMPG lipid bilayer in a D_2O buffer solution with *ppp* and *ssp* polarization combinations, we are able to determine the molecular tilt angle θ of the terminal CH_3 group of the phospholipid alkyl chain by utilizing the well-established polarization intensity ratio method.[1-5] Briefly, the *ppp* polarization combination probes a linear combination of χ_{xxz} , χ_{xzx} , χ_{zxx} , and χ_{zzz} tensor elements, whereas the *ssp* polarization combination only probes the χ_{yyz} tensor element, as expressed by

$$\begin{aligned}\chi^{(2)}_{\text{eff},ppp} = &-L_{xx}(\omega)L_{xx}(\omega_1)L_{zz}(\omega_2)\cos\beta\cos\beta_1\sin\beta_2\chi_{xxz}\\ &-L_{xx}(\omega)L_{zz}(\omega_1)L_{xx}(\omega_2)\cos\beta\sin\beta_1\cos\beta_2\chi_{xzx}\\ &+L_{zz}(\omega)L_{xx}(\omega_1)L_{xx}(\omega_2)\sin\beta\cos\beta_1\cos\beta_2\chi_{zxx}\\ &+L_{zz}(\omega)L_{zz}(\omega_1)L_{zz}(\omega_2)\sin\beta\sin\beta_1\sin\beta_2\chi_{zzz}\end{aligned} \quad (1)$$

$$\chi^{(2)}_{\text{eff, }ssp} = L_{yy}(\omega)L_{yy}(\omega_1)L_{zz}(\omega_2)\sin\beta_2\chi_{yyz} \tag{2}$$

where L values are Fresnel factors based on the optical parameters of our experimental setup and β_x (x = 0, 1, 2) values are the angles of the IR, visible, and SFG beams.

We assume that the methyl group of interest has full C_{3v} symmetry. Therefore, the tensor elements of interest are defined by the following expressions for a C_{3v}-type group symmetric stretch as[4]

$$\chi^{(2)}_{xxz} = \chi^{(2)}_{yyz} = \frac{1}{2}N_s\beta_{ccc}\left[\left(1+R\right)\left\langle\cos\theta\right\rangle - \left(1-R\right)\left\langle\cos^3\theta\right\rangle\right] \tag{3}$$

$$\chi^{(2)}_{xzx} = \chi^{(2)}_{zxx} = \chi^{(2)}_{yzy} = \chi^{(2)}_{zyy} = \frac{1}{2}N_s\beta_{ccc}\left(1-R\right)\left[\left\langle\cos\theta\right\rangle - \left\langle\cos^3\theta\right\rangle\right] \tag{4}$$

$$\chi^{(2)}_{zzz} = N_s\beta_{ccc}\left[R\left\langle\cos\theta\right\rangle + \left(1-R\right)\left\langle\cos^3\theta\right\rangle\right] \tag{5}$$

where β is the hyperpolarizability tensor and R is the hyperpolarizability ratio which is based on the Raman depolarization ratio of the particular vibrational mode.

The molecular orientation at an interface is defined by three angles: the azimuthal spin about the surface normal ϕ, the "twist" angle ψ, and the "tilt" angle θ. However, depending on the system of interest, simplifications can be made for defining the orientation. To this end, it is assumed that the methyl group has full C_{3v} symmetry with azimuthal rotational symmetry on a rotationally isotropic surface. Therefore, integrating over ϕ and ψ results in a molecular orientation that is solely dependent on the tilt angle θ of the C_{3v} symmetry axis of the terminal methyl group from the surface normal. By analyzing *ppp* and *ssp* polarization combinations, we are effectively comparing the SFG signal of a specific oscillator perpendicular and parallel to the surface normal, respectively, in order to triangulate a molecular tilt angle θ. Conboy and coworkers used *sps* and *ssp* polarization combinations to obtain the molecular tilt angle of the alkyl terminal

methyl groups for partially deuterated supported lipid bilayers.[6] However, we find that we achieve greater spectral signal to noise with the *ppp* polarization combination for our system.

The recorded *ssp* and *ppp* spectra were first fit to four Lorentzian lineshapes with different phases depending on the type of stretch, and using previously published peak assignments of similar systems from Conboy and coworkers based on prior phospholipid studies.[7-11] Specifically, we fit the spectra to account for the uncoupled terminal CH_3 group symmetric stretch around 2875 cm^{-1}, the Fermi resonance of the CH_2 symmetric stretch around 2900 cm^{-1}, an in-phase peak near 2965 cm^{-1} that may be due to the N–CH_3 symmetric stretch, and an out-of-phase peak near 2980 cm^{-1} that we attribute to the CH_3 asymmetric stretch. Through this peak fitting procedure we extract amplitude values, χ_{ppp} and χ_{ssp}, for a particular stretch. We carried out multiple peak fitting trials in order to obtain a point estimate of approximately 0.44 ± 0.01 for the the *ppp*/*ssp* amplitude ratio for the terminal alkyl chain CH_3 symmetric stretch around 2875 cm^{-1}.

Next, we compute theoretical *ppp*/*ssp* amplitude ratios as a function of the molecular tilt angle. These computed values are based on the optical properties of the said system (Table S1) as well as the assumption that there is a monomodal Gaussian distribution ranging from 1-40° (at FWHM).

Table S1. Reported optical parameters and their respective references used in computing theoretical χ_{ppp}/χ_{ssp} for the orientation analysis of the terminal alkyl CH_3 group of the 9:1 DMPC/DMPG bilayer.

Parameter/Beam	IR	Visible	SFG
Incident Angles	38.02	29.12	---
Wavenumber, cm^{-1}	2875	12500	15375
η (silica)[67]	1.4065	1.4533	1.4565
η (air)[68]	1.000273	1.000275	1.0002763
η (interface)[65]	1.48	1.48	1.48

Conboy and coworkers report using δ-distribution functions for the orientation analysis of terminal alkyl CH_3 group of partially deuterated supported lipid bilayers.[7] We have successfully carried out orientation analyses assuming Gaussian distributions in previous work[2, 12] and we find that studies of well-ordered polymer systems suggest that Gaussian distribution functions are appropriate for determining molecular orientations over δ distribution functions.[13-14] For these computations we used an interfacial refractive index of approximately 1.48, which was obtained from isotropic refractive index values for supported lipid bilayers reported by Reimhult and coworkers.[15] We used a hyperpolarizability ratio value *R* of 1.99 based on the previously reported Raman depolarization ratio of the terminal CH_3 symmetric stretch.[16]

Assuming that all terminal alkyl CH_3 groups are pointing within 1° of each other, the molecular tilt angle is ~28° from the surface normal (Figure 5b in the main text), as determined by the interception of the black curve with the dashed red experimental amplitude ratio curve. By taking into account the standard error associated with our point estimate ratio through multiple fittings,

which is given in the supporting information, the tilt angle distribution can be expanded to approximately 15-35° from the surface normal. These values are in good agreement with previously reported terminal CH_3 tilt angles of similar lipid bilayers.[7] Orientation analyses such as this should be approached with caution, in that large molecular orientation distributions will often predict a tilt angle of approximately 39° (±2), as presented by Simpson and Rowlen.[17] This 'magic angle' is the result of interfacial or surface roughness, which will broaden the molecular orientation distribution, and therefore obtaining a tilt angle near this angle may not necessarily be the true orientation angle value. However, we find that our average point estimate of the molecular tilt angle is not within this range and is reliable.

2. Fluorescence Image Analysis

All fluorescence images evaluated for percentage of bright spots were analyzed using ImageJ.[18] After opening the tif file in ImageJ, the image was background subtracted using the subtract background function located under the Process tab. We chose a rolling ball radius of 100 pixels and selected OK. The threshold of the image was then adjusted under Image/Adjust/Threshold. For the threshold adjustment, we held the minimum value at 0 and corrected the maximum value to be between 95% and 99.5% to give the best match to the image, ensured that Default, B&W, and Dark background were chosen, and selected Apply. We then employed the Invert function under the Edit tab to yield the inverted image resulting in a white image with black dots, as shown in Figure S1. Images shown in Figures S1, S2, and S3 are each 69 μm x 69 μm and scale bars have been excluded in Figures S1, S2, and S3A to reflect accurate analytical procedures on raw images.

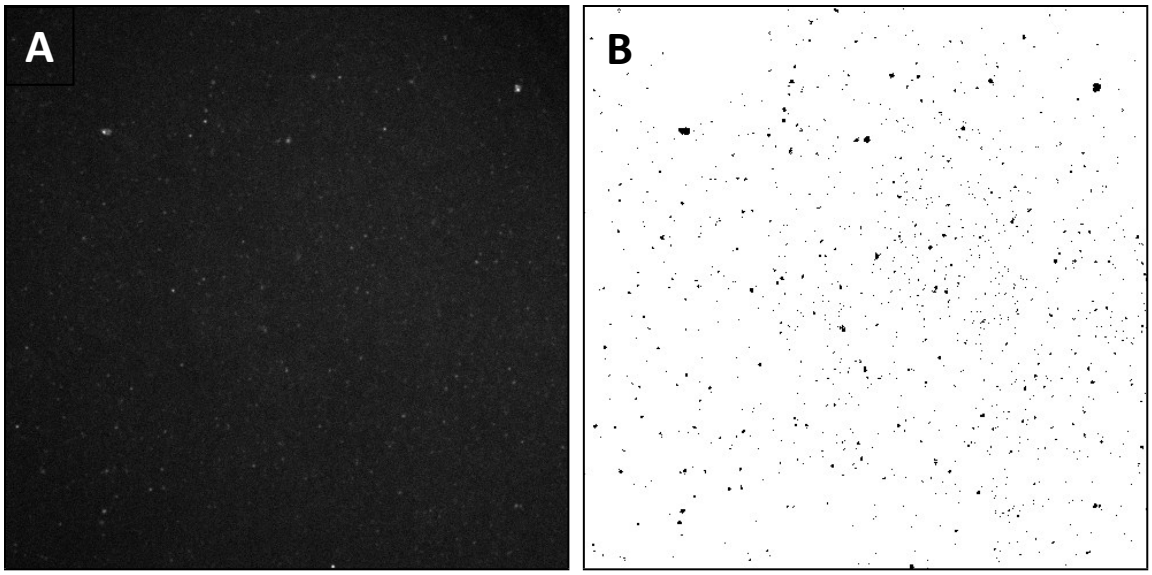

Figure S1. (A) Original fluorescence image of a DMPC bilayer doped with 0.01% Topfluor PC. (B) Same image after analysis in ImageJ in preparation for particle count analysis.

Next, we utilized the Analyze Particles feature under the Analyze tab, ensuring that the Size selected was 0 to Infinity, Circularity was set to 0.00-1.00, Show: Nothing, and that the following options were checked: Display results, Clear results, Summarize, Add to Manager. After clicking OK, the results were displayed in a Summary table, as well as the Regions of Interest in the ROI manager. The Summary table included the total particle count, total particle area (in square pixels) and percent area of particles. The main parameter of interest described in the main text is the percent area. Under the ROI manager window, we selected the Show All function, but made sure to deselect the Show Labels. The Show All function allowed us to view the areas ImageJ selected to be included in the total count and area of the Analyze Particles function. These particles were outlined in yellow, as shown in Figure S2.

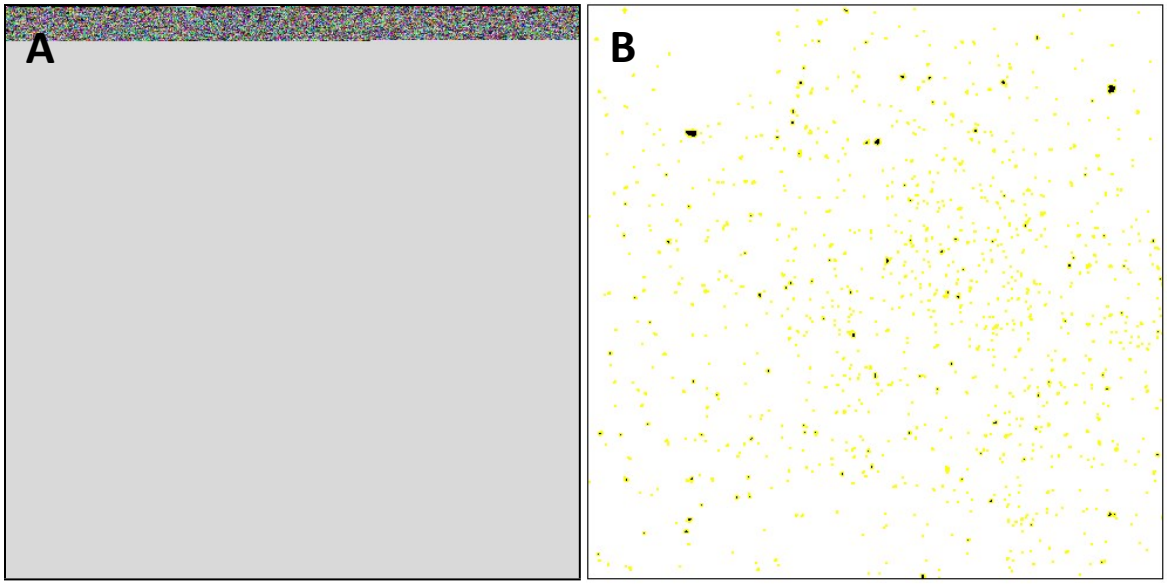

Figure S2. (A) Fluorescence image of DMPC bilayer doped with 0.01% Topfluor PC after analysis in ImageJ in preparation for particle count analysis. (B) Same image after particle count analysis depicting all particles counted by ImageJ circled in yellow.

To convert the image to closely reflect what was observed on the microscope, the image was opened in ImageJ and background subtracted as described above. Next, we changed to the green Lookup Table (LUT), which can be selected under Image/Lookup Tables/Green. We adjusted the Brightness/Contrast under Image/Adjust/Brightness/Contrast such that the minimum value remained at zero, and the maximum value was at the leading right edge of the tail (typically around 8000, but image-dependent). The chosen brightness/contrast adjustment was selected to best represent the image viewed on the microscope and applied to the image. We then added the calibration bar under Analyze/Tools/Calibration Bar with the following entries: Location: Upper Right, Fill Color: White, Label Color: Black, Number of Labels: 5, Decimal Places: 0, Font Size: 12, Zoom factor: 1.0, with Overlay selected and clicked OK. After the calibration bar was

added, we set the scale by choosing Analyze/Set Scale and entering the following values based upon microscope calibrations: Distance in pixels: 0.1412, Known distance: 1, Pixel aspect ratio: 1.0, Unit of length: um and clicking OK. We then added the scale bar using Analyze/Tools/Scale Bar with the following entries: Width in μm: 10, Height in pixels: 4, Font size: 14, Color: White, Background: None, Location: Lower Right with Bold Text selected. An example of the image before and after image processing is shown in Figure S3.

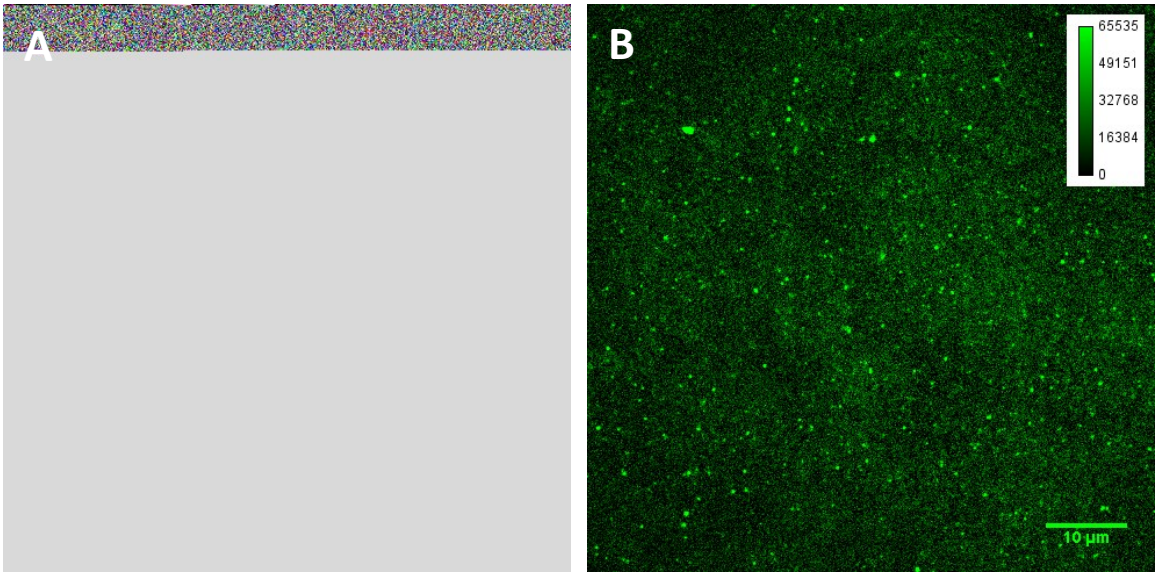

Figure S3. (A) Fluorescence image of DMPC bilayer doped with 0.01% Topfluor PC after analysis in ImageJ in preparation for particle count analysis. (B) Same image after ImageJ processing for best match to what was observed on the microscope.

Fluorescence Recovery After Photobleaching (FRAP) Analysis

FRAP analysis was carried out using the simFRAP plugin for ImageJ.[19] simFrap plugin information can be found at https://imagej.nih.gov/ij/plugins/sim-frap/index.html.

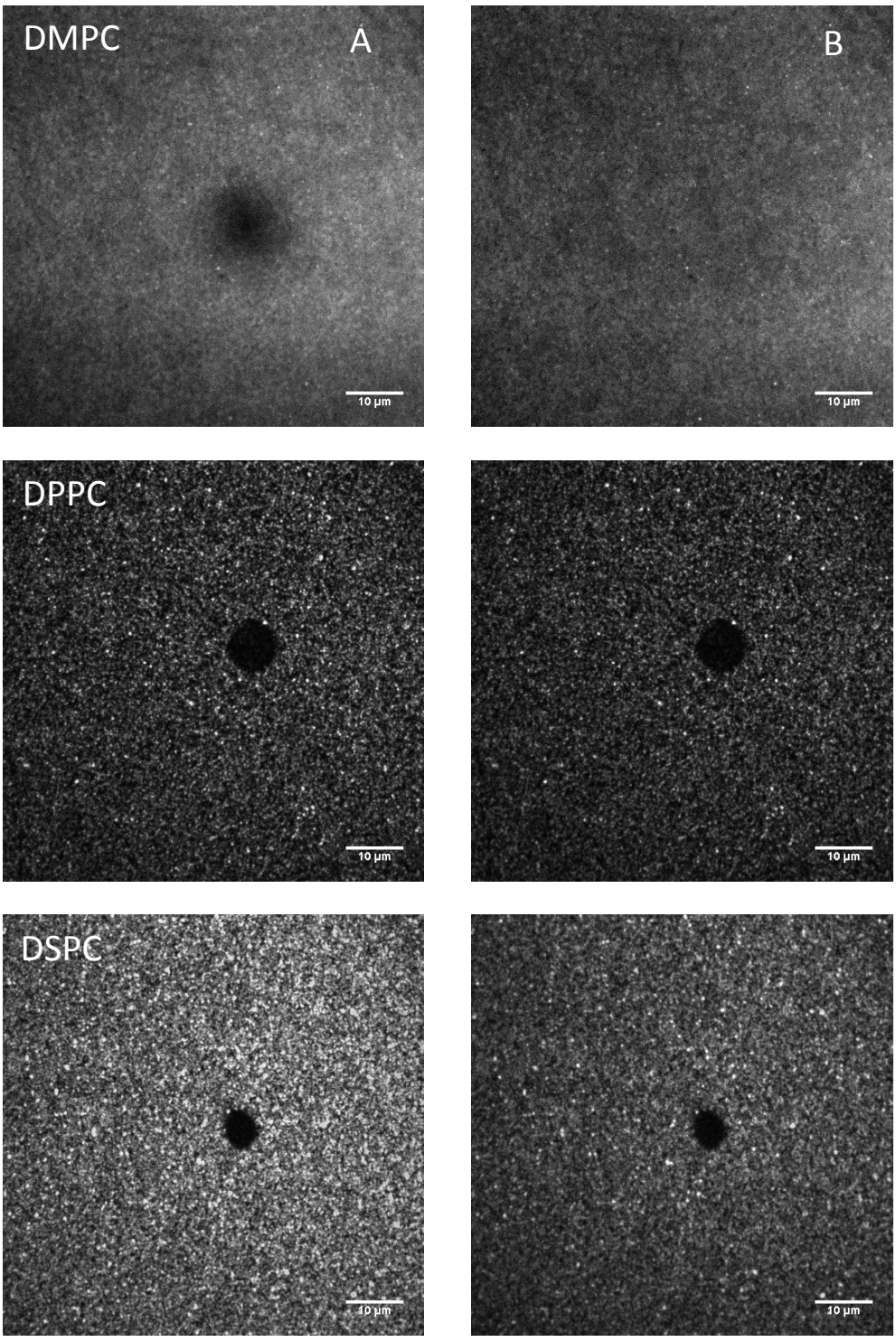

Figure S4. Representative FRAP images immediately after bleach (A) for DMPC, DPPC, DSPC (top to bottom) and later (B) DMPC after 80 s, DPPC after 80 s, DSPC after 300 s. Scale bars are 10 µm. Each bilayer was doped with 0.1% TopFluor PC.

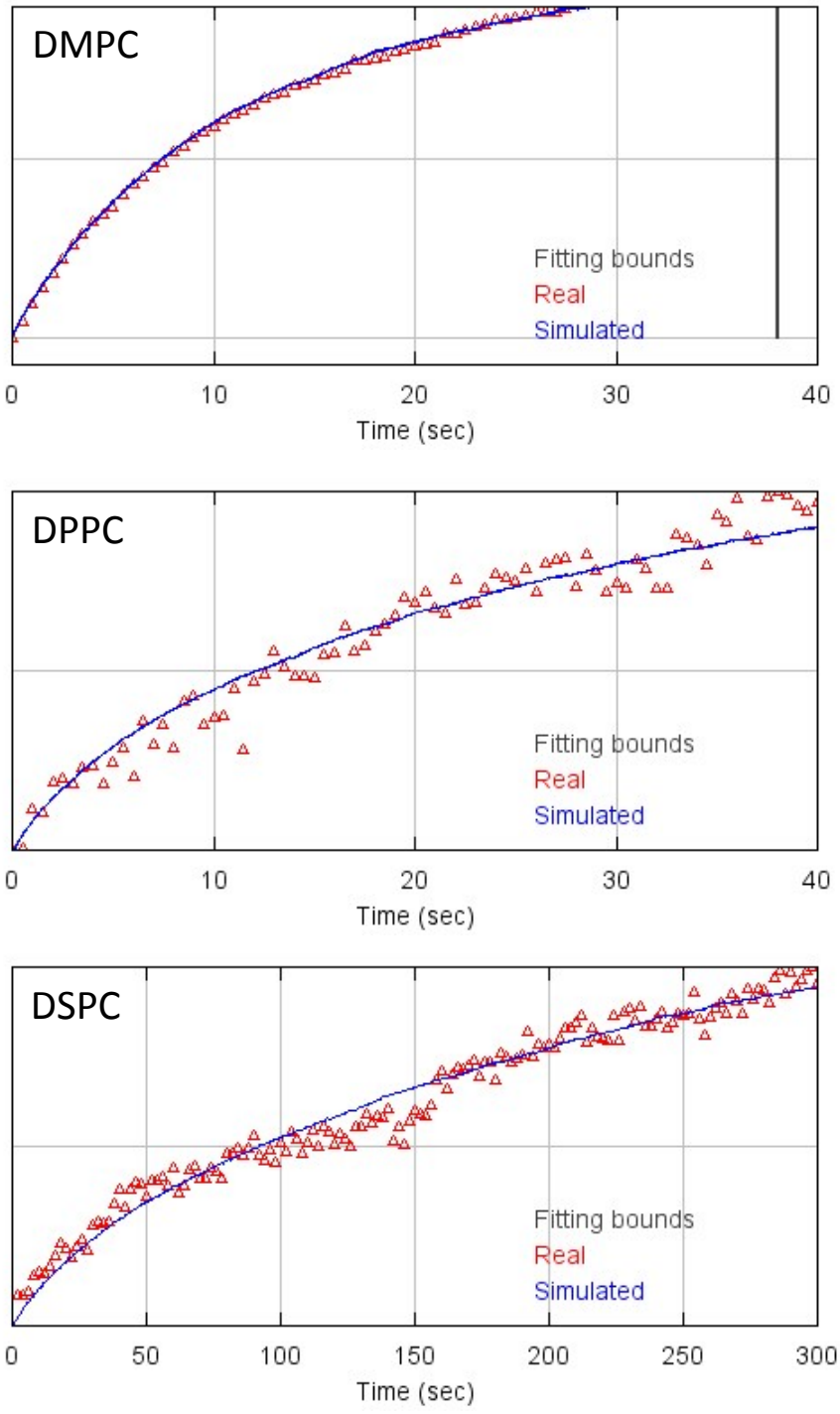

Figure S5. Representative simFRAP ImageJ plugin results. FRAP curves plotted as normalized fluorescence intensity as a function of time immediately after bleach for DMPC, DPPC, DSPC.

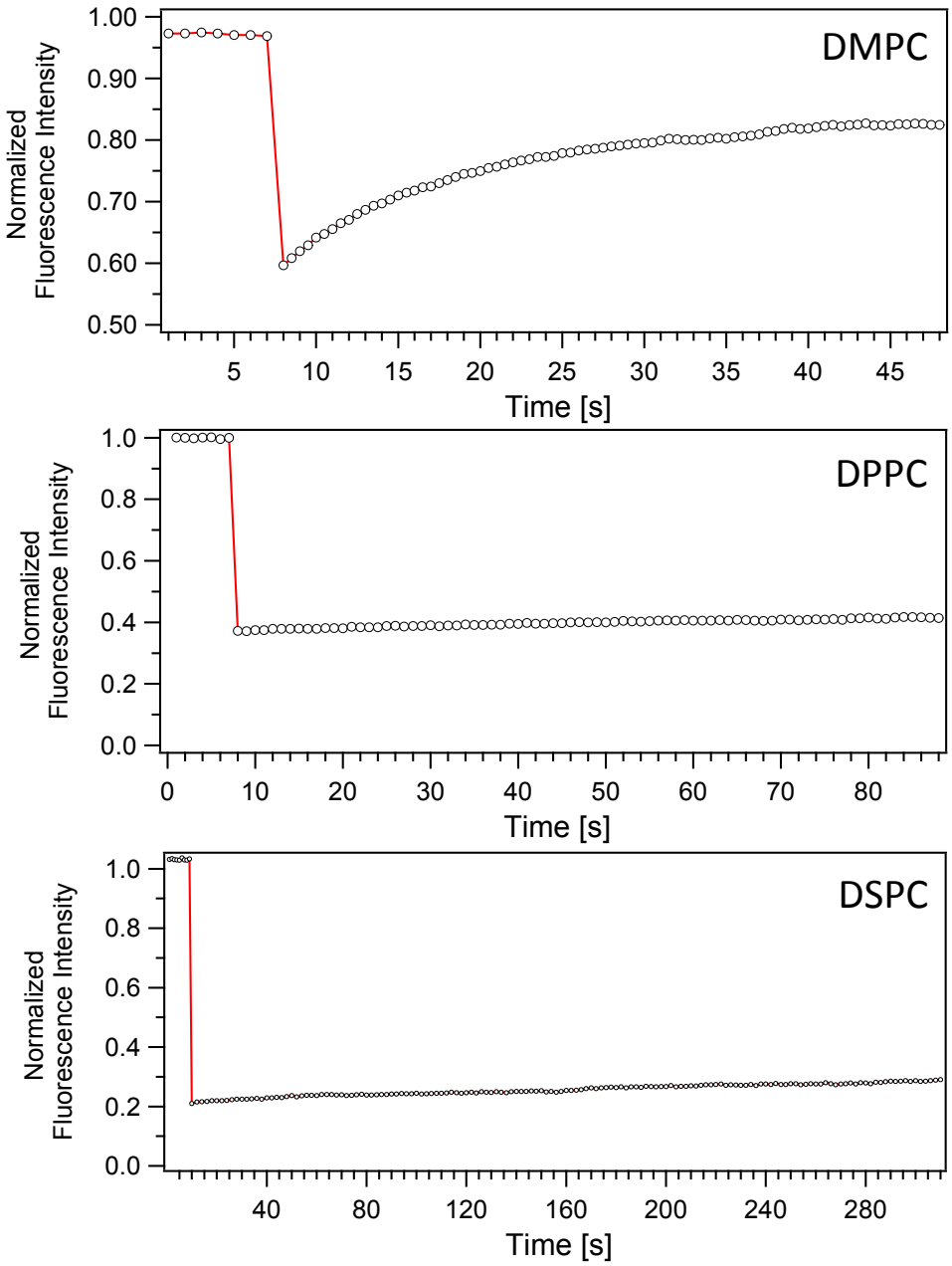

Figure S6. Normalized fluorescence intensity curves as a function of time for DMPC, DPPC, DSPC. To normalize each curve, the fluorescence intensity of the bleached area was divided by reference fluorescence intensity in order to account for photobleaching.

References

1. Buchbinder, A. M.; al, e., Method for Evaluating Vibrational Mode Assignments in Surface-Bound Cyclic Hydrocarbons Using Sum-Frequency Generation. *J. Phys. Chem. C* **2011**, *115*, 18284-18294.

2. Ebben, C. J.; Strick, B. F.; Upshur, M. A.; Chase, H. M.; Achtyl, J. L.; Thomson, R. J.; Geiger, F. M., Towards the Identification of Molecular Constituents Associated with the Surfaces of Isoprene-Derived Secondary Organic Aerosol (Soa) Particles. *Atmospheric Chemistry and Physics* **2014**, *14*, 2303-2314.

3. Moad, A. J.; Simpson, G. J., A Unified Treatment of Selection Rules and Symmetry Relations for Sum-Frequency and Second Harmonic Spectroscopies. *J. Phys. Chem. B* **2004**, *108*, 3548-3562.

4. Wang, H.-F.; Gan, W.; Lu, R.; Rao, Y.; Wu, B.-H., Quantitative Spectral and Orientational Analysis in Surface Sum Frequency Generation Vibrational Spectroscopy (Sfg-Vs). *International Reviews in Physical Chemistry* **2005**, *24*, 191-256.

5. Xu, M.; Liu, D.; Allen, H. C., Ethylenediamine at Air/Liquid and Air/Silica Interfaces: Protonation Versus Hydrogen Bonding Investigated by Sum Frequency Generation Spectroscopy. *Environ. Sci. Technol.* **2006**, *40*, 1566-1572.

6. Liu, J.; Conboy, J. C., Structure of a Gel Phase Lipid Bilayer Prepared by the Langmuir−Blodgett/Langmuir-Schaefer Method Characterized by Sum-Frequency Vibrational Spectroscopy. *Langmuir* **2005**, *21*, 9091-9097.

7. Liu, J.; Conboy, J. C., Structure of a Gel Phase Lipid Bilayer Prepared by the Langmuir-Blodgett/Langmuir-Schaefer Method Characterized by Sum-Frequency Vibrational Spectroscopy. *Langmuir* **2005**, *21*, 9091-9097.

8. Tamm, L. K.; Tatulian, S. A., *Q. Rev. Biophys.* **1997**, *30*, 365-429.

9. O'Leary, T. J.; Levin, I. W., *J. Phys. Chem.* **1984**, *88*, 1790-1796.

10. Snyder, R. G.; Strauss, H. L.; Elliger, C. A., *J. Phys. Chem.* **1982**, *86*, 5145-5150.

11. MacPhail, R. A.; Strauss, H. L.; Snyder, R. G.; Elliger, C. A., *J. Phys. Chem.* **1984**, *88*.

12. Achtyl, J. L.; Buchbinder, A. M.; Geiger, F. M., Hydrocarbon on Carbon: Coherent Vibrational Spectroscopy of Toluene on Graphite. *J. Phys. Chem. Lett.* **2012**, *3*, 280-282.

13. Chen, C.; Shen, Y. R.; Somorjai, G. A., Studies of Polymer Surfaces by Sum Frequency Generation Vibrational Spectroscopy. *Annu. Rev. Phys. Chem.* **2002**, *53*, 437-465.

14. Wei, X.; Zhuang, X.; Hong, S.-C.; Goto, T.; Shen, Y. R., Sum-Frequency Vibrational Spectroscopic Study of Rubbed Polymer Surface. *Phys. Rev. Lett.* **1999**, *82*, 4256-4259.

15. Mashaghi, A.; Swann, M.; Popplewell, J.; Textor, M.; Reimhult, E., Optical Anisotropy of Supported Lipid Structures Probed by Waveguide Spectroscopy and Its Application to Study of Supported Lipid Bilayer Formation Kinetics. *Analytical Chemistry* **2008**, *80*, 3666-3676.

16. Martin, J.; Montero, S., Raman Intensities of Ethane and Deuterated Derivatives. *J. Chem. Phys.* **1984**, *80*, 4610-4619.

17. Simpson, G. J.; Rowlen, K. L., An Shg Magic Angle: Dependence of Second Harmonic Generation Orientation Measurements on the Width of the Orientation Distribution. *J. Am. Chem. Soc.* **1999**, *121*, 2635-2636.

18. Schneider, C. A.; Rasband, W. S.; Eliceiri, K. W., Nih Image to Imagej: 25 Years of Image Analysis. *Nat Meth* **2012**, *9*, 671-675.

19. Blumenthal, D.; Goldstien, L.; Edidin, M.; Gheber, L. A., Universal Approach to Frap Analysis of Arbitrary Bleaching Patterns. *Scientific Reports* **2015**, *5*, 11655.